

Crystal structure, electronic, and magnetic properties of the bilayered rhodium oxide $\text{Sr}_3\text{Rh}_2\text{O}_7$

K. Yamaura,^{1,*} Q. Huang,^{2,3} D.P. Young,⁴ Y. Noguchi,⁵ and E. Takayama-Muromachi¹

¹*Superconducting Materials Center, National Institute for Materials Science, 1-1 Namiki, Tsukuba, Ibaraki 305-0044, Japan*

²*NIST Center for Neutron Research, National Institute of Standards and Technology, Gaithersburg, Maryland 20899*

³*Department of Materials and Nuclear Engineering,
University of Maryland, College Park, Maryland 20742*

⁴*Department of Physics and Astronomy, Louisiana State University, Baton Rouge, LA 70803*

⁵*Advanced Materials Laboratory, National Institute for Materials Science, 1-1 Namiki, Tsukuba, Ibaraki 305-0044, Japan*

(Dated: November 20, 2018)

The bilayered rhodium oxide $\text{Sr}_3\text{Rh}_2\text{O}_7$ was synthesized by high-pressure and high-temperature heating techniques. The single-phase polycrystalline sample of $\text{Sr}_3\text{Rh}_2\text{O}_7$ was characterized by measurements of magnetic susceptibility, electrical resistivity, specific heat, and thermopower. The structural characteristics were investigated by powder neutron diffraction study. The rhodium oxide $\text{Sr}_3\text{Rh}_2\text{O}_7$ [$Bbcb$, $a = 5.4744(8)$ Å, $b = 5.4716(9)$ Å, $c = 20.875(2)$ Å] is isostructural to the metamagnetic metal $\text{Sr}_3\text{Ru}_2\text{O}_7$, with five $4d$ electrons per Rh, which is electronically equivalent to the hypothetic bilayered ruthenium oxide, where one electron per Ru is doped into the Ru-327 unit. The present data show the rhodium oxide $\text{Sr}_3\text{Rh}_2\text{O}_7$ to be metallic with enhanced paramagnetism, similar to $\text{Sr}_3\text{Ru}_2\text{O}_7$. However, neither manifest contributions from spin fluctuations nor any traces of a metamagnetic transition were found within the studied range from 2 K to 390 K below 70 kOe.

PACS numbers: 75.50.-y

I. INTRODUCTION

The layered ruthenium oxides Sr_2RuO_4 , $\text{Sr}_3\text{Ru}_2\text{O}_7$, and the perovskites SrRuO_3 and CaRuO_3 , have attracted much attentions during the last several years primarily because these systems allow quantum phase transitions in clean metals¹ to be addressed experimentally.^{2,3,4,5} The appearances of novel transitions associated with the correlated $4d$ electrons continues to stir up significant issues within the condensed matter community. The layered member Sr_2RuO_4 , for example, enters a superconducting state at about 1 K in association with a rather unusual spin-triplet type electron-pairing, clearly at odds with predictions of conventional s -wave superconductivity.^{6,7} The bilayered member, $\text{Sr}_3\text{Ru}_2\text{O}_7$, shows non-Fermi liquid transport in the vicinity of a metamagnetic transition at high magnetic field and low temperature, suggesting that the scattering rate of the conduction electrons may be influenced by quantum fluctuations, as opposed to more conventional thermal fluctuations.^{8,9,10,11,12} Finally, data suggest that a quantum critical point exists in the solid solution $\text{Sr}_{1-x}\text{Ca}_x\text{RuO}_3$ for $x \sim 0.7$ between ferromagnetic (Sr-side) and nearly ferromagnetic (Ca-side) ordered states.^{13,14,15,16,17,18}

These materials have provided experimental opportunities to study criticality of correlated electrons in the vicinity of the quantum critical points.^{8,9,10,11,12} The present status of investigations of quantum phase transitions and criticality seem far behind that of the conventional transitions that are driven by thermal fluctuations.^{2,3,4,5} In order to promote progress in the studies of quantum phase transitions and criticality in clean metals, and to answer many open questions aroused thus far, we need further opportunities to study these is-

sues experimentally. Searching for a new class of materials which show quantum critical behavior within realizable magnetic, pressure, or chemical ranges, should be encouraged. High-quality single crystals of these materials, if available, would be highly desirable for experimental investigations.

We have been synthesizing the variety of compounds in the Sr-Rh(IV) oxide system, where Rh is expected to be $4d^5(t_{2g}^5e_g^0)$, by applying high-temperature and high-pressure techniques at typically 6 GPa and 1500 °C.¹⁹ Besides the counted members of the strontium-rhodium system,^{20,21,22,23} the perovskite-type compound was recently obtained by quenching to room temperature at elevated pressure.¹⁹ The formation of SrRhO_3 was an excellent example of what can be achieved by high-pressure techniques – no compounds at the ratio $\text{Sr:Rh} = 1:1$ had ever been reported until the high-pressure experiment. While the Sr substitution for $\text{LaRh}^{3+}\text{O}_3$ was studied by a regular solid-state-reaction technique at ambient pressure; it was then found that the solubility limit of Sr at the La site was at most 10 %, and the solid solution remained semiconducting in the very narrow region.²⁴ It is then clear that the formation of the 100 % end-member SrRhO_3 goes far beyond the limit achieved by the regular synthesis study, and it is indicative of the dramatic effectiveness of the high-pressure experiment. This synthesis technique can be expected to uncover further novel electronic materials in addition to SrRhO_3 .

The magnetic and electrical properties of SrRhO_3 were qualitatively similar of those observed in the analogous ruthenium oxide CaRuO_3 , the latter being a nearly ordered ferromagnetic metal that is probably influenced by spin-fluctuations.^{13,14,15,16,17,18} We had therefore expected unusual electronic properties in the unforeseen

compounds in the rhodium oxide system, as well as the analogous ruthenium oxides. We have focused our attention to obtaining further novel materials in the Sr-Rh-O space, and thus far, the Ruddlesden-Popper-type member $\text{Sr}_3\text{Rh}_2\text{O}_7$ was found. In this paper we present data from neutron diffraction study, magnetic and electrical measurements on a polycrystalline sample of this new phase, and the results are compared to the ruthenium analogue.

II. EXPERIMENTAL

The polycrystalline sample of $\text{Sr}_3\text{Rh}_2\text{O}_7$ was prepared as follows. The fine and pure ($\geq 99.9\%$) powders of SrO_2 , Rh_2O_3 , and Rh were mixed at the compositions $\text{Sr}_3\text{Rh}_2\text{O}_{7+z}$, where $z = 0.0$ and 0.1 . Approximately 0.2 grams of each stoichiometry was placed into a platinum capsule and then compressed at 6 GPa in a high-pressure apparatus, which was originally developed in our laboratory.²⁵ The sample was then heated at $1500\text{ }^\circ\text{C}$ for 1 hr and quenched to room temperature before releasing the pressure. The quality of the products was investigated by means of powder x-ray diffraction ($\text{CuK}\alpha$). The x-ray profile was carefully obtained at room temperature using the high-resolution-powder diffractometer (RINT-2000 system, developed by RIGAKU, CO), which was equipped with a graphite monochromator on the counter side. We found that the both samples were of high quality; there were no significant impurities in either product, and no remarkable difference between them. The x-ray pattern for the powder sample at $z = 0.0$ is shown in Fig.1. A quasi-tetragonal cell with $a = 5.474(1)\text{ \AA}$ and $c = 20.88(1)\text{ \AA}$ was tentatively applied to the data, and a clear assignment of (hkl) numbers to all the major peaks was obtained, indicating the high quality of the sample. The one probable impurity phase (less than 1%) was SrRhO_3 .¹⁹ The major phase in the samples could be reasonably assigned to $\text{Sr}_3\text{Rh}_2\text{O}_7$, of which there are no known records in the literature.

Possible oxygen vacancies in the compound were quantitatively investigated in detail by thermogravimetric analysis. Approximately 30 milligrams of the $z = 0.0$ powder was slowly heated at $5\text{ }^\circ\text{C}/\text{min}$ in a gas mixture (3% hydrogen in argon) and held at $800\text{ }^\circ\text{C}$ until the weight reduction became saturated. Calculated oxygen composition from the weight loss data was 7.01 per formula unit, indicating good oxygen stoichiometry.

Another sample of $\text{Sr}_3\text{Rh}_2\text{O}_7$, prepared at identical synthesis condition, was used for structural study by means of neutron diffraction. The powder neutron data of powder sample of $\text{Sr}_3\text{Rh}_2\text{O}_7$ (~ 0.2 grams) were collected at room temperature using the BT-1 high-resolution powder diffractometer at the NIST Center for Neutron Research, employing a $\text{Cu}(311)$ monochromator to produce a monochromatic neutron beam of wavelength 1.5396 \AA . Collimators with horizontal divergences of $15'$, $20'$, and $7'$ of arc were used before and after

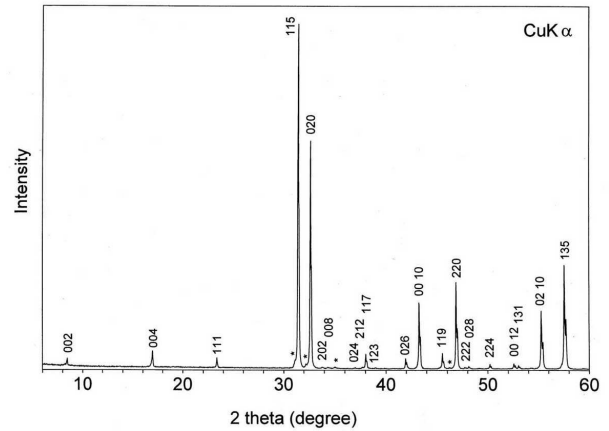


FIG. 1: Powder x-ray diffraction profile ($\text{CuK}\alpha$) of $\text{Sr}_3\text{Rh}_2\text{O}_7$, obtained at room temperature. A tentatively applied quasi-tetragonal unit cell with $a = 5.474(1)\text{ \AA}$ and $c = 20.88(1)\text{ \AA}$ yields a clear assignment of (hkl) numbers to almost all peaks, indicating quality of the sample. Unindexed peaks are marked by stars.

the monochromator, and after the sample, respectively. The intensities were measured in steps of 0.05° in the 2θ range 3° – 168° . The structural parameters were refined using the program GSAS.²⁶ The neutron scattering amplitudes used in the refinements were 0.702 , 0.593 , and 0.581 ($\times 10^{-12}\text{ cm}$) for Sr, Rh, and O, respectively.

The magnetic properties of the sample ($z = 0.0$) were studied in a commercial apparatus (Quantum Design, MPMS-XL system) between 2 K and 390 K . The magnetic susceptibility data were collected at 1 kOe and 70 kOe , and magnetization curves were recorded between -70 kOe and 70 kOe after cooling the sample at each 2 K , 5 K and 50 K . The electrical resistivity was measured by a conventional ac-four-terminal technique at zero field and at 70 kOe . The ac-gauge current was 0.1 mA at 30 Hz . The selected sample ($z = 0.0$) was cut out into a bar shape, and the each face was polished with aluminum-oxide-lapping film. In order to decrease the contact resistance with the sample, gold pads ($\sim 200\text{ nm}$ in thickness) were deposited at four locations along the bar, and silver epoxy was used to fix platinum wires ($\sim 30\text{ }\mu\text{m}\phi$) at each gold terminal. The contact resistance at the four terminals was less than 8 ohm .

III. RESULTS AND DISCUSSIONS

The crystal structure of the title compound was investigated by means of neutron powder diffraction at room temperature. In an effort to maximize the homogeneity of the sample, only one pellet was subjected to the neutron study rather than a mixture of multiple pellets, even though the total sample mass was far below the regular level. The degree of local structure distortions, such as cooperative rotations of metal-oxygen octahedra and fre-

TABLE I: Structure parameters of $\text{Sr}_3\text{Rh}_2\text{O}_7$ at room temperature. Space group: $Bbcb$ (No.68). The lattice parameters are $a = 5.4744(8)$ Å, $b = 5.4716(9)$ Å, and $c = 20.875(2)$ Å. The volume of the orthorhombic unit cell is $625.3(2)$ Å³. $Z = 4$. The calculated density is 6.17 g/cm³. The constraints on the analysis: $y[\text{O}(3)] = -x[\text{O}(3)] + 1/2$, $x[\text{O}(3')] = 1 - x[\text{O}(3)]$, $y[\text{O}(3')] = -y[\text{O}(3)]$, $z[\text{O}(3')] = z[\text{O}(3)]$, $B[\text{O}(3')] = B[\text{O}(3)]$, and $n[\text{O}(3')] = 1 - n[\text{O}(3)]$. The R factors were 5.42% (R_p) and 6.47% (R_{wp}). Selected bond distances (Å) and angles (°) are shown in the bottom part.

Atom	Site	x	y	z	$B(\text{\AA}^2)$	n
Sr(1)	4a	1/4	1/4	0	0.5(2)	1
Sr(2)	8e	1/4	1/4	0.1867(3)	0.8(2)	1
Rh	8e	1/4	1/4	0.4013(4)	0.1(2)	1
O(1)	4b	1/4	1/4	1/2	1.2(3)	1
O(2)	8e	1/4	1/4	0.3062(4)	0.6(2)	1
O(3)	16i	0.5473(5)	-0.0473(5)	0.0973(4)	0.6(1)	0.92(2)
O(3')	16i	0.4527(5)	0.0473(5)	0.0973(4)	0.6(1)	0.08(2)
Sr(1)–O(1)	×2	2.7358(4)		Rh–O(1)		2.060(8)
Sr(1)–O(1)	×2	2.7372(4)		Rh–O(2)		1.985(12)
Sr(1)–O(3)	×4	3.069(7)		Rh–O(3)	×2	1.9694(8)
Sr(1)–O(3)	×4	2.566(8)		Rh–O(3)	×2	1.9697(8)
Sr(2)–O(2)		2.494(11)		O(1)–Rh–O(3)		89.1(4)
Sr(2)–O(2)	×2	2.7411(7)		O(2)–Rh–O(3)		90.9(4)
Sr(2)–O(2)	×2	2.7398(7)		O(1)–Rh–O(2)		180
Sr(2)–O(3)	×2	2.44(1)		Rh–O(3)–Rh		158.5(2)
Sr(2)–O(3)	×2	2.964(8)				

quency of stacking faults in the layered structure, may depend sensitively on the synthesis conditions. Technical problems, such as small sample volume within the high-pressure apparatus and uncertainties in the maximum temperature during the heating process, could contribute to small variations in sample quality. Measuring an individual pellet by neutron powder diffraction was intended to preclude possible errors in the analysis of the local structural distortion. The structural distortion was naturally expected in $\text{Sr}_3\text{Rh}_2\text{O}_7$ based on the analogy with $\text{Sr}_3\text{Ru}_2\text{O}_7$, since the ionic size of ${}^{\text{VI}}\text{Rh}^{4+}$ (0.60 Å)²⁷ is very close to that of ${}^{\text{VI}}\text{Ru}^{4+}$ (0.62 Å).^{28,29,30} Furthermore, the expected distortions were hard to detect with normal x-ray diffraction.

The pellet as made in a platinum capsule was highly polished with a fine sandpaper to reduce possible Pt contamination. The pellet (~0.2 grams) was then finely ground for the neutron diffraction study. The neutron data were collected at room temperature for approximately one and a half days; the profile is shown in Fig.2. Although the sample powder was exposed to the neutron beam for many hours, the intensity did not reach normal levels due to the small sample mass. It was, however, sufficient enough to deduce structural information from the data. The small impurity contribution, found in the x-ray study, and possible magnetic contributions were not investigated due to the low intensity level.

The major concern in the structure investigation of the title compound was whether a cooperative rotation of the metal-oxygen octahedra occurs as is found in the analogous $\text{Sr}_3\text{Ru}_2\text{O}_7$.^{28,29,30} In the study of the *ruthenium* oxide by means of neutron diffraction, eight independent modes for the cooperative rotation ($Bbcm$, $Bbcb$, $Bbmm$, $Bmcm$, $P4_2/mnm$, $P4_2/mcm$, $P4_2/m$, $B112/m$), com-

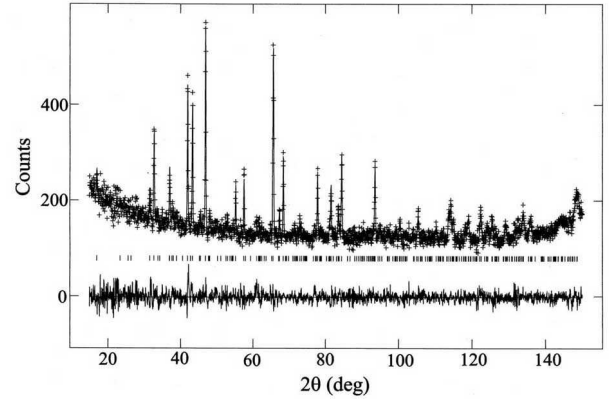


FIG. 2: Neutron diffraction profile of the powder sample (~0.2 grams) of $\text{Sr}_3\text{Rh}_2\text{O}_7$, obtained at room temperature at $\lambda = 1.5396$ Å. Vertical bars indicate expected peak positions for the orthorhombic ($Bbcb$) structure model. The difference between the orthorhombic model (solid lines) and the data (crosses) is shown below the bars column. Although intensity statistic appeared to be rather lower due to the small sample mass, the analysis succeeded in obtaining a high-quality solution.

bination of some of those, and the rotation-free mode ($I4/mmm$) were tested. It was found that the $Bbcb$ mode resulted in the highest quality of the profile analysis.²⁸ Here, in the analysis of the profile of $\text{Sr}_3\text{Rh}_2\text{O}_7$, we first applied the $Bbcb$ mode and found it to produce reasonable solutions ($R_p = 5.42\%$, $R_{wp} = 6.47\%$) to describe the cooperative rotation of RhO_6 octahedra in $\text{Sr}_3\text{Rh}_2\text{O}_7$. Although the $Bbcb$ mode is the most likely structural distortion in $\text{Sr}_3\text{Ru}_2\text{O}_7$, other lower symmetry modes, as mentioned above, are still possible. Unfortunately,

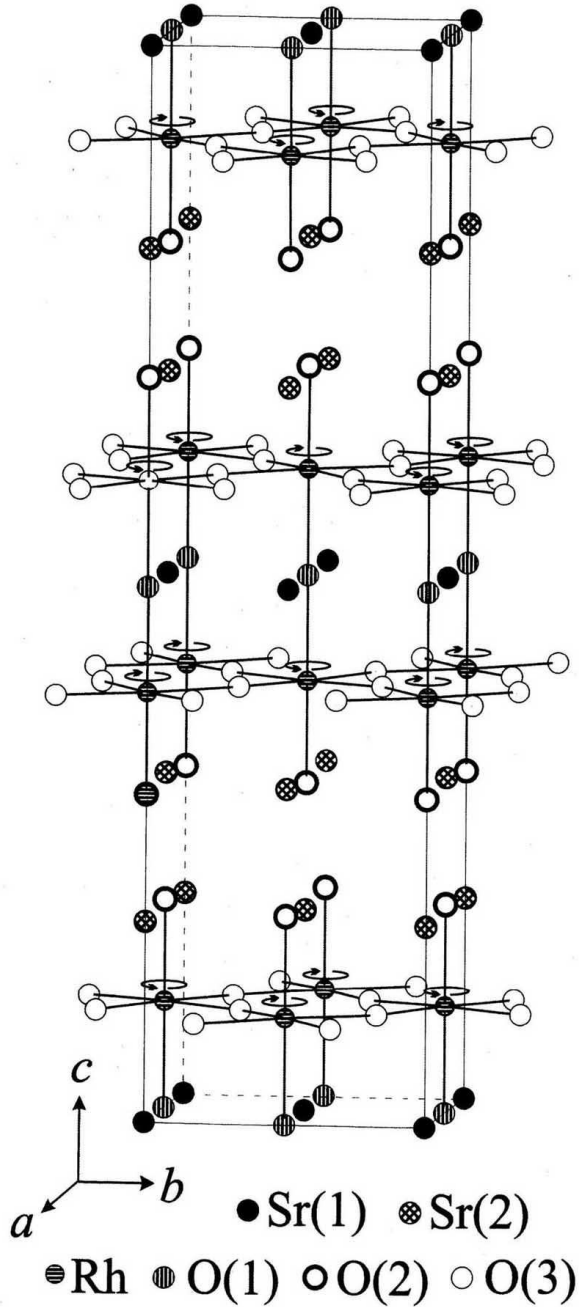


FIG. 3: Structural view of $\text{Sr}_3\text{Rh}_2\text{O}_7$. Fine lines signifies the orthorhombic unit cell. Cooperative rotations along c -axis of the RhO_6 octahedra are indicated by circular arrows.

the low intensity of the data in the present study made it difficult to completely dismiss the other modes. Detailed analysis of the issue is left for future work, in which further progress of the high-pressure-synthesis technique will allow us to obtain a larger amount of highly homogenized sample.

Probable stacking faults were examined by introducing the $\text{O}(3')$ elements with some constraints (caption of Table I), as was done for $\text{Sr}_3\text{Ru}_2\text{O}_7$. As a result, sig-

nificant improvements in the overall fit were obtained ($<\sim 2\%$ in R values). The estimated occupancy of $\text{O}(3')$ was $\sim 8\%$, indicating the frequency of the stacking faults. The estimated structural parameters of $\text{Sr}_3\text{Rh}_2\text{O}_7$, and selected bond distance and angles, are arranged in Table I. The isotropic atomic displacement parameter (B) of the rhodium ion (8e-site) is rather unusual, possibly because the low level of the intensity statistics reduced reliability of the thermal parameters somewhat. We believe further structure studies, on not only a larger amount of sample powder, but also a single crystal of $\text{Sr}_3\text{Rh}_2\text{O}_7$, might provide much more reliable data.

The structure of $\text{Sr}_3\text{Rh}_2\text{O}_7$ is shown in Fig.3. The directions of rotation are indicated by circular arrows. The rotation results in the bond angle of $\text{Rh}-\text{O}(3)-\text{Rh}$ being 159 degrees rather than 180 degrees for an ideally rotation-free structure. The rotation angle of RhO_6 octahedra along c -axis is 10.5 degrees, which is slightly greater than that of RuO_6 octahedra in the analogous $\text{Sr}_3\text{Ru}_2\text{O}_7$ (6.8 degrees).²⁸ A general diagram for the degree of distortion in Ruddlesden-Popper-type compounds $A_3M_2\text{O}_7$ (A : alkaline and/or rare earth metal; M : transition metal) was proposed, in which the real members of $A_3M_2\text{O}_7$ were divided into two categories: one with and one without distortions associated with cooperative rotations of the MO_6 octahedra.²⁸ A criterion named “zero strain line” was established for judging which category each member should belong to. The combination of radii of ${}^{VI}\text{Rh}^{4+}$ (0.60 Å) and ${}^{XII}\text{Sr}^{2+}$ (1.44 Å) in $\text{Sr}_3\text{Rh}_2\text{O}_7$ ²⁷ yields a point below the “zero strain line” in the proposed diagram, implying that $\text{Sr}_3\text{Rh}_2\text{O}_7$ should be in the distortion-free category. This classification for the $\text{Sr}_3\text{Rh}_2\text{O}_7$ case appears to be incorrect as dictated by the data in the present study.²⁸ Characteristics of chemical bonds may play a pivotal role in the distortion process, and their consideration may be necessary if a complete diagram is to be developed.

The electrical resistivity data of the polycrystalline sample of $\text{Sr}_3\text{Rh}_2\text{O}_7$ are shown in Fig.4. Temperature and magnetic field dependence was studied between 2 K and 390 K. The resistivity at room temperature is ~ 75 mΩ·cm, which is approximately one magnitude larger than that of the 3D SrRhO_3 ¹⁹ and one magnitude smaller than that of the 2D Sr_2RhO_4 , which is a barely metallic conductor.^{31,32} The series of the rhodium oxides $\text{Sr}_{n+1}\text{Rh}_n\text{O}_{3n+1}$ ($n = 1, 2$, and ∞) consist of solely homovalent elements including Rh^{4+} ($4d^5$: may be in the low-spin configuration $t_{2g}^5 e_g^0$), and all of them clearly show metallic character, while the electronic dimensionality varies from two to three. This suggests that the metallic character is developed with increasing electronic dimensionality. Further studies involving band structure calculations could be significant in revealing how essential the dimensionality is to the electronic transport of the rhodium oxide series. A small magnetic field dependence was found at low temperature ($<\sim 20\text{K}$) as shown in the inset of Fig.4. Future studies on single crystals may provide insight into the mechanism responsible for

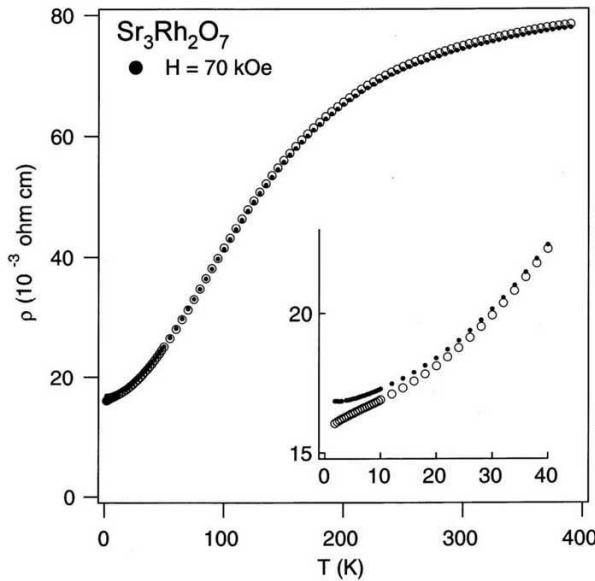


FIG. 4: Temperature dependence of the electrical resistivity of the polycrystalline $\text{Sr}_3\text{Rh}_2\text{O}_7$ at zero field and 70 kOe. Inset shows an expansion of the low-temperature portion.

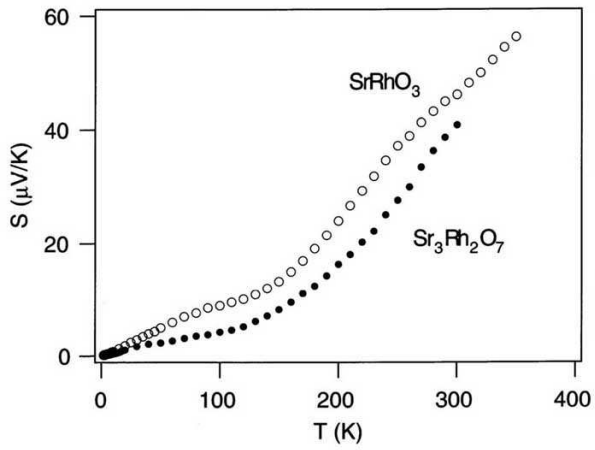


FIG. 5: Thermoelectric property of the polycrystalline $\text{Sr}_3\text{Rh}_2\text{O}_7$ and SrRhO_3 . The data for the perovskite compound were taken from a previous report.³³

the positive magnetoresistance.

The Seebeck coefficient of the title compound was measured and compared with that of the perovskite SrRhO_3 (Fig.5).³³ The Seebeck coefficient of Sr_2RhO_4 , reported previously, was approximately $+40\mu\text{V/K}$ at room temperature and decreases linearly to approach zero upon cooling.³² The data of all three compounds (Sr_2RhO_4 , $\text{Sr}_3\text{Rh}_2\text{O}_7$, and SrRhO_3) are qualitatively consistent with the metallic conductivity observed for each, and indicate that the sign of the majority carriers is positive in the metallic conducting state. Among the Seebeck coefficient of the three compounds, it is hard to find a remarkable difference qualitatively and quantitatively, in con-

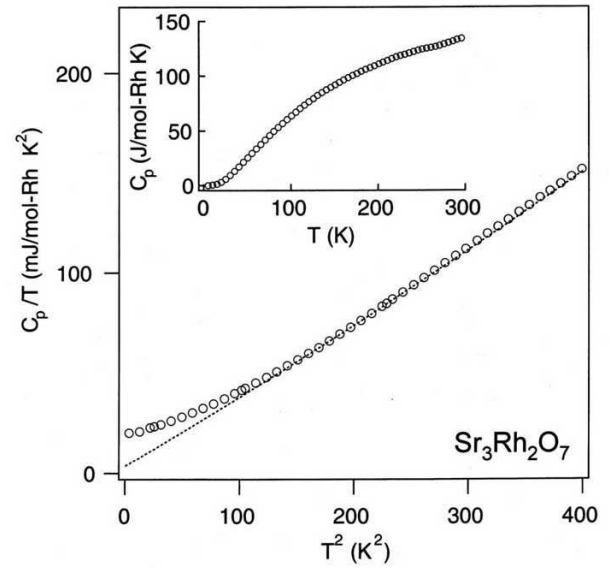


FIG. 6: Specific heat of the polycrystalline $\text{Sr}_3\text{Rh}_2\text{O}_7$. The data are plotted in C_p/T vs T^2 (main panel) and C_p vs T (inset) forms. The dotted curve represents a fit to the data (details are in the text).

trast to the case of the resistivity data. Although a small change in slope in the Seebeck coefficient was observed in both $\text{Sr}_3\text{Rh}_2\text{O}_7$ and SrRhO_3 at approximately 150 K (Fig.5), there were, however, no corresponding anomalies in other transport data around that temperature. The change may be structurally related, and further studies of the temperature dependence of structural distortions may help to address the issue.

The specific heat data are plotted as C_p/T vs T^2 (main panel) and C_p vs T (inset) in Fig.6. The electronic and lattice contributions to the specific heat can be isolated from the data in the main panel by using the following low-temperature form ($T \ll \Theta_D$):

$$\frac{C_V}{T} = \gamma + \frac{12\pi^4}{5} N k_B \left(\frac{1}{\Theta_D^3} \right) T^2,$$

where Θ_D , γ , β , k_B , and N are Debye temperature, Sommerfeld's coefficient, Boltzmann's constant, and Avogadro's number, respectively. The two independent parameters, Θ_D and γ , which indicate physical characteristics of the compound, were estimated by a least-square method in the linear range between 150 K^2 and 450 K^2 ; we obtained $\Theta_D \sim 172\text{ K}$ and $\gamma \sim -0.00199\text{ J}\cdot\text{mol-Rh}^{-1}\cdot\text{K}^{-2}$. The estimation of both γ and Θ_D was, however, not solid; a small degree of variations was found. For example, when a T^4 term was added to the equation, the fits achieved were $\Theta_D \sim 180\text{ K}$, γ of $\sim 0.00365\text{ J}\cdot\text{mol-Rh}^{-1}\cdot\text{K}^{-2}$, and β (the coefficient of the T^4 term) of $7.93 \times 10^{-8}\text{ J}\cdot\text{mol-Rh}^{-1}\cdot\text{K}^{-6}$, as indicated by the dotted curve. Although it is technically difficult to determine a precise value for γ , it should, however, be very small in contrast to that of the metallic SrRhO_3 ($\gamma =$

7.6 mJ/mol-Rh/K²).¹⁹ The depressed metallic character of the bilayered $\text{Sr}_3\text{Rh}_2\text{O}_7$ is reflective in the very small value of γ . It would be interesting to compare the value of γ_{band} , computed from the density of states at the Fermi level by means of band-structure calculations, with and without consideration of spin polarization. In the above analysis we assumed that C_p was approximately equal to C_v because it was in the low temperature limit.

As expected from the Debye temperature (170 K–180 K) of the layered oxide $\text{Sr}_3\text{Rh}_2\text{O}_7$, even within the studied temperature range, the specific heat approaches the high-temperature limit, roughly calculated to be $\sim 150 \text{ J}\cdot\text{mol-Rh}^{-1}\cdot\text{K}^{-1}$ [6(atoms per unit cell) $\times 3$ (dimensionality per atom) $\times k_{\text{B}}\text{N}$ (Boltzmann and Avogadro's constants)]. The Debye temperature of $\text{Sr}_3\text{Rh}_2\text{O}_7$ is close to that of the perovskite SrRhO_3 ($\Theta_{\text{D}} \sim 190$ K). To our knowledge, the Debye temperature of Sr_2RhO_4 has not been reported.

A small component, which appears in the low-temperature limit of the C_p/T vs T^2 curve (the data points gradually apart from the fitting curve on cooling), is probably due to a magnetic origin. In order to make clear the origin of the probable magnetic component, several magnetic models were tested on the specific heat data. The studies, however, did not yield a clear assignment of magnetic model to the origin because there were still too many possibilities related to a nuclear Schottky specific heat, an empirical temperature-independent term, ferro- and antiferromagnetic spin fluctuations, and associations of some of those. As far as the present investigation goes, it was therefore unlikely to establish a clear picture with a reasonable sense to understand the appearance of the very small component in the low-temperature specific heat data.

Nearly-temperature-independent magnetic susceptibility data, measured between 2 K and 390 K, are shown in Fig. 7. The majority of the data could be characterized as Pauli paramagnetic with an enhanced $\chi(0)$. The $\chi(300)$ is approximately 1.0×10^{-3} emu/mol-Rh, nearly one magnitude larger than those of normal paramagnetic metals, including $\text{Rh(IV)}\text{O}_2$.^{34,35,36} This is a curious result, considering the very small γ -value estimated from the specific heat measurements. More will be said on this below. Alternatively, a layered spin system, despite the metallic character, is probable to account for the magnetic characteristics with the broad maximum at about 200 K as is the case for the Sr doped La_2CuO_4 .³⁷ Further studies to explore probable localized magnetic moments should be of interest. The steep upturn in low temperature at 1 kOe is due to a small concentration of magnetic impurities, which could be well fit to a Curie-Weiss law; the magnetic parameters were $C = 0.00194$ emu K/mol-Rh (Curie constant), $\theta_W = -0.1462$ K (Weiss temperature), and $\chi_0 = 9.21 \times 10^{-4}$ emu/mol-Rh (temperature-independent susceptibility). The rather small value of θ_W , less than 1 K, indicates that the diluted moments are free from magnetic interactions, as is often the cases. The M vs H curves measured at 2 K, 5 K and 50 K are shown

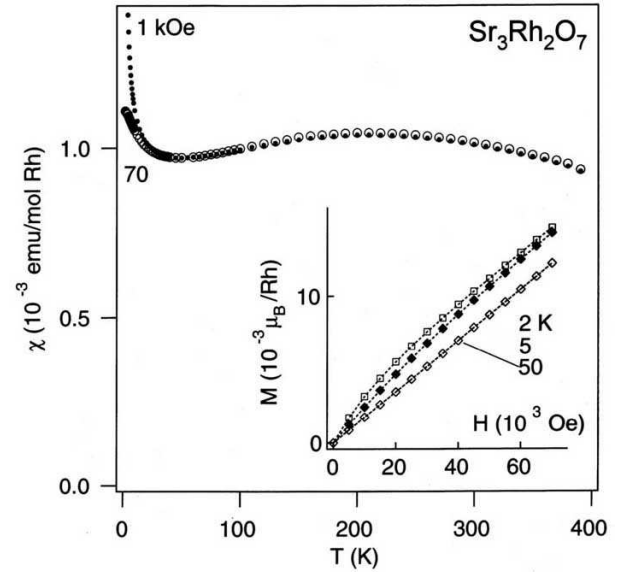


FIG. 7: Temperature dependence of the magnetic susceptibility of the polycrystalline $\text{Sr}_3\text{Rh}_2\text{O}_7$ at 1 kOe and 70 kOe on cooling, and applied magnetic field dependence of the magnetization (inset) at 2 K, 5 K and 50 K.

in the inset of Fig. 7. The small component ($\sim 0.001\mu_{\text{B}}$ at 70 kOe and 5 K), which is superimposed on the paramagnetic background, is probably due to the magnetic impurity outlined above. While a metamagnetic transition was clearly found in the analogous $\text{Sr}_3\text{Ru}_2\text{O}_7$ at ~ 50 kOe and 2.8 K in fields both parallel and perpendicular to the c -axis of a single crystal,⁹ no trace of one could be seen in the data of $\text{Sr}_3\text{Rh}_2\text{O}_7$ even at 2.0 K. Such a transition may be shifted to higher fields in the Rh sample, and in order to investigate this possibility, a pulsed high-magnetic-field study at low temperature is scheduled for $\text{Sr}_3\text{Rh}_2\text{O}_7$.

IV. CONCLUSIONS

High-pressure synthesis techniques have been utilized in an effort to add to the variety of experimental systems currently being used in the study of quantum phase transitions and criticality. The systematic synthesis experiments performed thus far on the Rh^{4+} ($4d^5 : t_{2g}^5 e_g^0$, expected) oxide system have revealed a new class of Ruddlesden-Popper phases $\text{Sr}_{n+1}\text{Rh}_n\text{O}_{3n+1}$ ($n = 1$ [ref. 31 and 32], 2 [this work], and ∞ [ref. 19]). The neutron diffraction study clearly reveals that the new metallic rhodium oxide, $\text{Sr}_3\text{Rh}_2\text{O}_7$, is isostructural to the ruthenium oxide $\text{Sr}_3\text{Ru}_2\text{O}_7$, which has received much recent attention due to its intriguing quantum characteristics. The magnetic and transport data presented here, however, do not indicate clear contributions from quantum fluctuations in the studied range of temperature and magnetic field, in contrast to what was observed in the ruthenium compound.^{38,39} Since the Curie-Weiss-like be-

havior was not seen (except for the impurity term) even in the high-temperature portion of the magnetic susceptibility data, the self-consistent renormalization theory of spin fluctuations for both antiferro- and ferromagnetic nearly-ordered magnetic metals may not be applicable to the present magnetic and specific heat data.^{40,41}

While the magnetic susceptibility data of $\text{Sr}_3\text{Rh}_2\text{O}_7$ suggest a rather large density of states at the Fermi level (similar to what was observed in SrRhO_3), the linear term in the heat capacity is, however, remarkably small – on the order of semimetals like Bi and Sb. The resistivity is about 10 times larger than that of SrRhO_3 , qualitatively consistent with the rather small γ . It is possible that the influence of disorder in the polycrystalline sample at a level undetectable by the techniques in the present study masks the intrinsic nature of ideally clean $\text{Sr}_3\text{Rh}_2\text{O}_7$. In the studies of the ruthenium oxides, for example, the quantum properties were found to be rather fragile to such disorder.^{42,43} Further information, including carrier density, degree of disorder, band structure, would prove useful in clearly identifying the intrinsic properties of $\text{Sr}_3\text{Rh}_2\text{O}_7$. High-quality single crystals of sufficient size for electronic transport studies synthesized in the high-pressure cell would afford the opportunity of further investigations of $\text{Sr}_3\text{Rh}_2\text{O}_7$ at a much deeper level.

In the ruthenium oxide family, much effort have been spent in searching for new superconducting compounds, but only the 214 phase is a superconductor. One member found recently (non-superconducting) is the double-layered $\text{Sr}_3\text{Ru}_2\text{O}_7\text{F}_2$, where Ru ions are pentavalent.⁴⁴ One electronic hole per formula unit was formally doped

into metallic $\text{Sr}_3\text{Ru}_2\text{O}_7$, and an ordered magnetic moment ($\sim 1\mu_B$ per Ru) was found below about 185 K. On the other hand, $\text{Sr}_3\text{Rh}_2\text{O}_7$ has five 4d electrons per formula unit, i.e. one electron per Ru is hypothetically doped into $\text{Sr}_3\text{Ru}_2\text{O}_7$, and no localized moments observed. The following is a general description of the three bilayered compounds: The localized character at the $4d^3$ layered compound gets weakened at $4d^4$ and becomes much more itinerant at $4d^5$. The overall comprehensive picture about the electronic structure of various 4d compounds has probably not yet been established. Further studies, including theoretical considerations and a systematic study of isovalent and aliovalent chemical doping to the series $\text{Sr}_{n+1}\text{Rh}_n\text{O}_{3n+1}$ would be of interest. Further progress of the high-pressure-synthesis technique may allow future investigations of new and unforeseen electronic materials those are potentially intriguing.

Acknowledgments

We wish to thank Dr. M. Akaishi (NIMS) and Dr. S. Yamaoka (NIMS) for their advice on the high-pressure experiments. This research was supported in part by Superconducting Materials Research Project, administrated by the Ministry of Education, Culture, Sports, Science and Technology of Japan. One of us (K.Y.) was supported by the Domestic Research Fellowship, administrated by the Japan Society for the Promotion of Science.

* E-mail at:YAMAURA.Kazunari@nims.go.jp;
Fax.:+81-298-58-5650

¹ The words “clean metal” hereby mean a metal in the low disorder limit.

² G.R. Stewart, Rev. Mod. Phys. **73**, 797 (2001).

³ S. Sachdev, *Quantum phase transitions*, Cambridge University Press, Cambridge, 1999.

⁴ S.L. Sondhi, S.M. Girvin, J.P. Carini, and D. Shahar, Rev. Mod. Phys. **69**, 315 (1997).

⁵ J.A. Hertz, Phys. Rev. B **14**, 1165 (1976).

⁶ K. Izawa, H. Takahashi, H. Yamaguchi, Yuji Matsuda, M. Suzuki, T. Sasaki, T. Fukase, Y. Yoshida, R. Settai, and Y. Onuki, Phys. Rev. Lett. **86**, 2653 (2001).

⁷ K. Ishida, Y. Kitaoka, K. Asayama, S. Ikeda, S. Nishizaki, Y. Maeno, K. Yoshida, and T. Fujita, Phys. Rev. B **56**, R505 (1997).

⁸ S.A. Grigera, R.S. Perry, A.J. Schofield, M. Chiao, S.R. Julian, G.G. Lonzarich, S.I. Ikeda, Y. Maeno, A.J. Millis, and A.P. Mackenzie, Science **294**, 329 (2001).

⁹ R.S. Perry, L.M. Galvin, S.A. Grigera, L. Capogna, A.J. Schofield, A.P. Mackenzie, M. Chiao, S.R. Julian, S.I. Ikeda, S. Nakatsuji, Y. Maeno, and C. Pfleiderer, Phys. Rev. Lett. **86**, 2661 (2001).

¹⁰ D.J. Singh and I.I. Mazin, Phys. Rev. B **63**, 165101 (2001).

¹¹ S.I. Ikeda, Y. Maeno, S. Nakatsuji, M. Kosaka, and Y. Uwatoko, Phys. Rev. B **62**, R6089 (2000).

¹² A.V. Puchkov, M.C. Schabel, D.N. Basov, T. Startseva, G. Cao, T. Timusk, and Z.-X. Shen, Phys. Rev. Lett. **81**, 2747 (1998).

¹³ K. Yoshimura, T. Imai, T. Kiyama, K.R. Thurber, A.W. Hunt, and K. Kosuge, Phys. Rev. Lett. **83**, 4397 (1999).

¹⁴ T. Kiyama, K. Yoshimura, K. Kosuge, H. Mitamura, and T. Goto, J. Phys. Soc. Jpn. **68**, 3372 (1999).

¹⁵ T. Kiyama, K. Yoshimura, K. Kosuge, H. Michor, and G. Hilscher, J. Phys. Soc. Jpn. **67**, 307 (1998).

¹⁶ G. Cao, S. McCall, M. Shepard, J.E. Crow, and R.P. Guertin, Phys. Rev. B **56**, 321 (1997).

¹⁷ T. He and R.J. Cava, Phys. Rev. B **63**, 172403 (2001).

¹⁸ T. He, Q. Huang, and R.J. Cava, Phys. Rev. B **63**, 024402 (2000).

¹⁹ K. Yamaura and E. Takayama-Muromachi, Phys. Rev. B **64**, 224424 (2001).

²⁰ K.E. Stitzer, A. El Abed, J. Darriet, and H.-C. zur Loyer, J. Am. Chem. Soc. **123**, 8790 (2001).

²¹ J.R. Plaisier, A.A.C. van Vliet, and D.J.W. Ijdo, J. Alloys Comp. **314**, 56 (2000).

²² J.B. Claridge and H.-C. zur Loyer, Chem. Mater. **10**, 2320 (1998).

²³ R. Horyń, Z. Bukowski, M. Wołczyrz, and A.J. Zaleski, *J. Alloys Comp.* **262-263**, 267 (1997).

²⁴ T. Nakamura, T. Shimura M. Itoh, and Y. Takeda, *J. Solid State Chem.* **103**, 523 (1993).

²⁵ S. Yamaoka, M. Akaishi, H. Kanda, T. Osawa, T. Taniguchi, H. Sei, and O. Fukunaga, *J. High Pressure Inst. Jpn.* **30**, 249 (1992).

²⁶ A.C. Larson and R.B. Von Dreele, Los Alamos National Laboratory Report No. LAUR086-748 (1990).

²⁷ R. D. Shannon, *Acta Crystallogr. Sec. A* **32**, 751 (1976).

²⁸ H. Shaked, J.D. Jorgensen, O. Chmaissem, S. Ikeda, and Y. Maeno, *J. Solid State Chem.* **154**, 361 (2000).

²⁹ H. Shaked, J.D. Jorgensen, S. Short, O. Chmaissem, S.-I. Ikeda, and Y. Maeno, *Phy. Rev. B* **62**, 8725 (2000).

³⁰ Q. Huang, J.W. Lynn, R.W. Erwin, J. Jarupatrakorn, and R.J. Cava, *Phy. Rev. B* **58**, 8515 (1998).

³¹ M. Itoh, T. Shimura, Y. Inaguma, and Y. Morii, *J. Solid State Chem.* **118**, 206 (2000).

³² T. Shimura, M. Itoh, Y. Inaguma, and T. Nakamura, *Phy. Rev. B* **49**, 5591 (1994).

³³ K. Yamaura, D. P. Young, and E. Takayama-Muromachi, in the 2002 MRS Spring Meeting, San Francisco, California (in press).

³⁴ H. Kojima, R.S. Tebble, and D.E.G. Williams, *Proc. Phys. Soc. London* **A260**, 237 (1961).

³⁵ D.W. Budworth, F.E. Hoare, and J. Preston, *Proc. Phys. Soc. London* **A257**, 250 (1960).

³⁶ F.E. Hoare and J.C. Walling, *Proc. Phys. Soc. London, Sect. B* **64**, 337 (1951).

³⁷ M. Imada, A. Fujimori, and Y. Tokura, *Rev. Mod. Phys.* **70**, 1039 (1998).

³⁸ S. Ikeda, Y. Maeno, and T. Fujita, *Phy. Rev. B* **57**, 978 (1998).

³⁹ R.J. Cava, H.W. Zandbergen, J.J. Krajewski, W.F. Peck Jr., B. Batlogg, S. Carter, R.M. Fleming, O. Zhou, and L.W. Rupp Jr., *J. Solid State Chem.* **116**, 141 (1995).

⁴⁰ T. Moriya, *Spin Fluctuations in Itinerant Electron Magnetism*, edited by Manuel Cardona (Springer-Verlag, 1985).

⁴¹ T. Moriya and K. Ueda, *Adv. Phys.* **49**, 555 (2000).

⁴² L. Capogna, A.P. Mackenzie, R.S. Perry, S.A. Grigera, L.M. Galvin, P.Raychaudhuri, A.J. Schofield, C.S. Alexander, G. Cao, S.R. Julian, and Y. Maeno, *Phy. Rev. Lett.* **88**, 076602 (2002).

⁴³ A.P. Mackenzie, R.K.W. Haselwimmer, A.W. Tyler, G.G. Lonzarich, Y. Mori, S. Nishizaki, and Y. Maeno, *Phy. Rev. Lett.* **80**, 161 (1998).

⁴⁴ R.K. Li and C. Greaves, *Phy. Rev. B* **62**, 3811 (2000).